Electron localization–delocalization in mixed-valence iron dimers

ARTICLE *in* CHEMICAL PHYSICS LETTERS · APRIL 2000

Impact Factor: 1.9 · DOI: 10.1016/S0009-2614(00)00210-4

7 April 2000

ELSEVIER

Chemical Physics Letters 320 (2000) 295–302

CHEMICAL PHYSICS LETTERS

www.elsevier.nl/locate/cplett

Electron localization–delocalization in mixed-valence iron dimers

S.M. Ostrovsky [a], R. Werner [a], K. Nag [b], W. Haase [a,*]

[a] *Institute of Physical Chemistry, Darmstadt University of Technology, Petersenstraße 20, D-64287 Darmstadt, Germany*
[b] *Department of Chemistry, Indian Association for the Cultivation of Science, Jadavpur, Calcutta 700 032, India*

Received 9 July 1999; in final form 3 February 2000

Abstract

Two mixed-valence iron dimers, $[L^1Fe_2(\mu\text{-}OAc)_2](ClO_4)$ and $[L^1Fe_2(\mu\text{-}OBz)(OBz)(H_2O)](ClO_4)$, were investigated. The temperature dependence of the effective magnetic moments and the position and shape of the intervalence absorption bands were calculated using a Hamiltonian taking into account isotropic exchange interaction, double exchange, Zeeman interaction, zero-field splitting for the ground state and vibronic coupling with the PKS out-of-phase mode. The similarities and differences of the investigated compounds were explained on the basis of analysis of the adiabatic potentials. The behaviour of both systems is determined by a strong competition between two main processes: double exchange interaction and vibronic coupling with PKS out-of-phase mode. Degree of delocalization of the itinerant extra electron was calculated at different values of temperature.

1. Introduction

Mixed-valence (MV) transition metal clusters are of great interest because of their unusual spectral and magnetic properties and the possibility to use these properties for studying the intramolecular electron transfer process in many biologically important compounds [1,2]. For instance, valence delocalized $[Fe_2S_2]^+$ pairs, where iron is in the formal oxidation state $+2.5$, were found in a variety of iron–sulfur clusters in ferredoxins. Because of this, a growing interest in the characterization, the modelling, as well as in the theoretical description of such compounds, exists [3–6]. However up to now, only a few completely valence delocalized, dinuclear, mixed-valent, iron complexes with oxygen as bridging atoms are known [7–12].

MV dimers are very convenient systems for better understanding the electron delocalization process because of the possibility of taking into account all relevant interactions. As it was shown [13,14], the energy levels of MV systems are not completely described by the isotropic exchange Hamiltonian ($\hat{H} = -2J\vec{S}_1\vec{S}_2$, where J is the isotropic exchange parameter). For the explanation of the properties of MV compounds it is necessary to take into consideration the double exchange interaction as well. In the case where the ground multielectron state is orbitally non-degenerated, the energy levels of the dimeric cluster are described by the well-known Eq. (1):

$$E_{\pm}(S) = -JS(S+1) \pm B\left(S+\tfrac{1}{2}\right), \qquad (1)$$

where B is the double exchange parameter, and S the total spin of the system. In multielectron MV dimers the itinerant extra electron is shown to produce a strong ferromagnetic effect through the double exchange mechanism [14].

* Corresponding author. Fax: +49-6151-16-4924; e-mail: haase@hrzpub.tu-darmstadt.de

0009-2614/00/$ - see front matter
PII: S0009-2614(00)00210-4

The moving electron strongly perturbs the ligand environment so the vibronic coupling plays a considerable role in MV systems, along with isotropic and double exchange interactions. The background for the consideration of the vibronic effects in this kind of systems was suggested by Piepho, Krausz and Schatz and became well-known as the PKS model [15–17]. The PKS model operates with the full-symmetric ('breathing') vibrations of the local environment of each ion of the cluster. The vibronic interaction with the out-of-phase breathing mode is relevant to the electron transfer process. Strong PKS interaction produces a localization effect.

The PKS model is not the only possibility of taking into account vibronic interactions in MV systems. Piepho [18,19] suggested a new vibronic coupling model for these type of compounds. In this model, multi-center vibrations are produced by the modulation of the intermetallic distances. As distinguished from the PKS-type of vibrations, this kind of vibronic coupling contributes to the electron delocalization effect, and thus produces a ferromagnetic effect in the MV dimers.

MV systems are traditionally classified by the degree of delocalization of the itinerant extra electron using the Robin and Day classification scheme [20]. These compounds can belong to valence trapped (Class I), partially delocalized (Class II) or fully delocalized (Class III) systems. This classification scheme is of fundamental importance for the chemical insight on MV compounds. The criteria of belonging to one of the three classes in the Robin and Day classification scheme have been formulated in the framework of the PKS model [16] as well as in the framework of the generalized model that takes into account the two mentioned different types of vibrations [21].

In this Letter we continue our work [10,11] on the detailed analysis of the two dinuclear mixed-valent Fe(II)–Fe(III) complexes, the experimental and theoretical investigation of their properties and the theoretical explanation of common features and differences in their magnetic behaviour.

2. Experimental part

The synthesis, crystal structure and Mössbauer data of compound **1** were described elsewhere [10]. The complex has a centrosymmetric geometry (space group: $P2_1/n$) with an Fe–Fe distance of 2.74 Å. Compound **2** was synthesized in the same way, using sodium benzoate instead of sodium acetate. The detailed crystal structure will be described elsewhere [22]. The complex is non- centrosymmetric with an increased Fe–Fe distance of 2.91 Å compared to **1**. The average distance between iron and the bridging phenolic oxygen atoms is different for both iron sites (2.064 and 2.018 Å, respectively). Schematic structures of both complexes are shown in Fig. 1. Detailed magnetic data of compound **2**, as well as Mössbauer and NIR spectroscopic data, can be found in Ref. [12].

Magnetic susceptibility of samples of **1** [10,11] and **2** [12] were recorded on a Faraday-type magnetometer consisting of a Cahn RG electrobalance, a Leyboldt Heraeus VNK 300 helium flux cryostat, and a Bruker BE25 magnet connected with a Bruker B–Mn 200/60 power supply in the temperature range 4.3–300 K. The applied magnetic field was ~0.5 T. Details of the apparatus have been described elsewere [23]. To prevent orientation effects of the microcrystalline sample by the magnetic field the measurements were carried out suspending the powdered complexes in a paraffin matrix and cooling down to liquid-helium temperature in zero field. The experimental susceptibility data were corrected for the underlying diamagnetism of the sample holder, of the paraffin matrix and of the compounds themselves.

The optical absorption spectra were recorded with a Cary 17 (Varian) spectrometer in the temperature

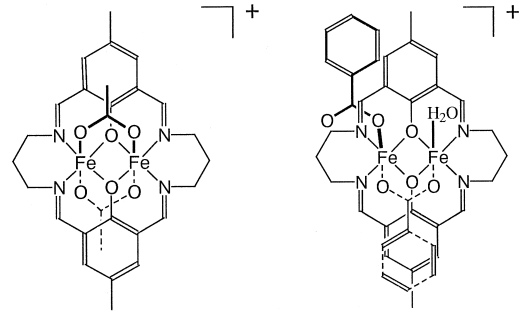

Fig. 1. Schematic structures of $[L^1Fe_2(\mu\text{-}OAc)_2]^+$ (left) and $[L^1Fe_2(\mu\text{-}OBz)(OBz)(H_2O)]^+$ (right).

range 85–300 K. For the NIR region a PbS detector was used, for the UV/Vis range a photomultiplier was applied. All spectra were obtained in a two-beam modus. Using this spectrometer the measurements were carried out [12] adjusting the two beams with the help of the monochromator slit, therefore the resolution of the spectra is a function of wavelength and absorption. At room temperature the resolution was always better than 5 nm. In the temperature range between 85 and 300 K a bathcryostat (Thor Cryogenics Series 100 Cryostat) was used and cooled with liquid nitrogen. The temperature was measured with a Fe–Au thermoelement. The quartz windows of the cryostat show absorption at 1382 and 2200 nm. In this temperature range the resolution was not as good due to the remarkable scattering effects caused by the potassium bromide pellets containing the samples (1 mg sample ground with 100 mg KBr and pressed with 10 t). The room temperature spectra were carried out in acetonitrile. Temperature-dependent NIR data of **1** and **2** are presented in [12]. The intervalence band was found at 8800 and 7250 cm^{-1} for **1** and **2**, respectively.

Raman measurements were carried out with a SPEX U 1000 Raman spectrometer and an argon ion laser.

A detailed description of all experimental data will be given elsewhere [22].

3. Data analysis

The detailed analysis of compound **1** has been done in Ref. [10] where magnetic behaviour of this system was explained without taking into account any vibronic interactions. Unfortunately, all attempts to describe in this way compound **2**, failed; however, both compounds have similar structure and chemical properties and we can expect that they must be described in the framework of the same theoretical model. To explain magnetic properties of both compounds we used the following Hamiltonian,

$$\hat{H} = -JS(S+1) + B\hat{T}_{AB} + \beta\{g_{\parallel}H_Z S_Z + g_{\perp}(H_X S_X + H_Y S_Y)\} + D_{gr}\{S_{grZ}^2 - \tfrac{1}{3}S_{gr}(S_{gr}+1)\} + \hat{O}_{vib} + \hat{W}_A, \quad (2)$$

where the first term is due to the isotropic exchange interaction, the second term describes the double exchange interaction, the third one is the Zeeman interaction, the fourth describes the zero-field splitting for the ground state (only the axial component, D_{gr}, of the zero-field splitting tensor is assumed to be non zero) and the fifth one is a vibronic part of the Hamiltonian. The last term in Eq. (2) takes into account the non equivalency of the sites A and B:

$$\hat{W}_A\psi_A^{SM}(r) = W\psi_A^{SM}(r), \ \hat{W}_A\psi_B^{SM}(r) = 0,$$

where $\psi_{A(B)}^{SM}(r)$ means the electronic wave function of the system, with the extra electron localized on centre A(B), S means the total spin of the system (M is the magnetic quantum number).

In our calculations we followed Ref. [17]. The eigenfunctions of (2) can be found in the following form,

$$\Phi_\nu^{SM}(r,q) = \psi_+^{SM}(r)\sum_{n=0}^{N} C_{\nu,n}^{+S}\chi_n(q) + \psi_-^{SM}(r)\sum_{n=0}^{N} C_{\nu,n}^{-S}\chi_n(q), \quad (3)$$

where $\psi_\pm^{SM}(r) = 2^{-1/2}\{\psi_A^{SM}(r) \pm \psi_B^{SM}(r)\}$ and $\chi_n(q)$ – means the harmonic oscillator function. All interactions in (2) cannot mix states of the system belonging to different values of the total spin. As a consequence, the full matrix of (2) splits into 5 blocks. Each of them corresponds to one of the total spin values. In general the rank of these blocks is infinite, but in practical calculations for moderate vibronic coupling it is enough to take into account in (3) only about a hundred low-lying vibronic levels for each value of the total spin, without significant loss of accuracy. For central symmetric compound **1** the full set of eigenfunctions (3) splits into two subsets (even and odd) that also reduce the rank of the matrix to be diagonalized for definition of $C_{\nu,n}^{+S}$ and $C_{\nu,n}^{-S}$ values.

Solid-state Raman spectra for both compounds are presented elsewhere [22]. In the limit of no coupling between bridging and terminal motions there are only six $(2N-6)$ metal–ligand vibrational degrees of freedom. Normal coordinate calculations for the

D_{2h} idealized symmetry system allow us to associate the observed spectra with the normal vibrations. The frequency of the PKS out-of-phase mode is ~ 310 cm^{-1}, which is in a good agreement with the values obtained in Ref. [6].

The position and the shape of the intervalence absorption band can then be calculated using eigenfunctions and eigenvalues of (2) and standard quantum mechanical methods. It should be mentioned that in the framework of the pure PKS model it is impossible to obtain a broad intervalence band for the fully delocalized compound **1** (Class III). The investigations of the regarded complex on the basis of the generalized vibronic model are in progress.

For compound **2** a very good agreement between theoretical and experimental curves (see Fig. 2) was achieved for the following set of parameters: the value of the double exchange parameter B was 600 cm^{-1}, the vibronic coupling parameter υ was $3.5\,\omega$ and $W = 400$ cm^{-1}. For compound **1** the corresponding values are: $B = 820$ cm^{-1} and $\upsilon = 3.5\,\omega$ (W is equal to 0, because compound **1** is a centrosymmetric complex). One can see that in the presence of vibronic coupling with the PKS out-of-phase mode, the position of the maximum of the intervalence absorption band does not correspond anymore to the $2(S_{gr} + \frac{1}{2})$ values of the double exchange parameter. To explain the physical properties of the system in this case, we need a smaller B-value (in our calculation for compound **1** $B = 820$ cm^{-1} compared with 940 cm^{-1} in Ref. [10] and the expected ~ 880 cm^{-1} [1]). Of course, the values of double exchange parameters, B, for both compounds are only approximated and can differ slightly from the real parameters of the systems. The values of the double exchange and the vibronic coupling parameter, obtained by this method were used for the calculation of magnetic properties of the investigated systems.

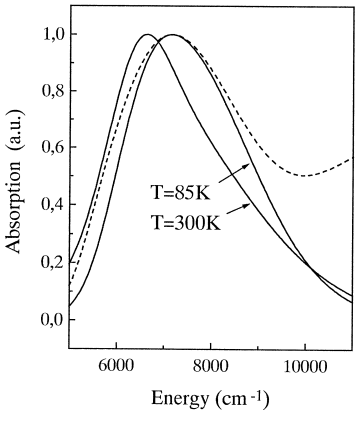

Fig. 2. Intervalence absorption band of compound **2** (dotted curve, $T = 85$ K) and theoretical fit (solid curves): $B = 600$ cm^{-1}, $\omega = 310$ cm^{-1}, $\upsilon = 3.5\,\omega$, $J = -22$ cm^{-1}, $W = 400$ cm^{-1}.

The temperature dependence of the magnetic behaviour can be computed using the well-known Van Vleck equation:

$$\chi_{\text{Van Vleck}}(T,\vartheta) = \frac{N\sum_S\sum_M\sum_{\nu=0}^{\infty}\left[\frac{\left(E^{(1)}_{SM}(\nu)\right)^2}{kT} - 2E^{(2)}_{SM}(\nu)\right]\exp\left(-\frac{E^{(0)}_{SM}(\nu)}{kT}\right)}{\sum_S\sum_M\sum_{\nu=0}^{\infty}\exp\left(-\frac{E^{(0)}_{SM}(\nu)}{kT}\right)}, \quad (4)$$

where $E^{(0)}_{SM}(\nu)$ is the energy of vibronic level ν in zero field, and $E^{(1)}_{SM}(\nu)$ and $E^{(2)}_{SM}(\nu)$ are first- and second-order Zeeman coefficients, respectively. The summation in (4) runs over all values of total spin, its projection and all vibronic levels. The magnetic susceptibility is a function of the angle ϑ between the applied magnetic field and the principal axis of the ZFS tensor (it is significant mostly for the low-temperature region) [24]. To find the powder-average magnetic susceptibility it is necessary to integrate Eq. (4) over ϑ:

$$\chi(T) = \frac{1}{2}\int_0^{\pi}\chi(T,\vartheta)\sin\vartheta\,\mathrm{d}\vartheta\,. \quad (5)$$

To characterize a measure of delocalization of the itinerant extra electron we have used two values: the probability distribution in the configuration space,

[1] The intervalence absorption band is peculiar to the mixed-valence compounds and is formed from the transitions between the states with the same spin value and different parity. In the case of neglecting any vibronic coupling the position of the maximum of this band corresponds to the transition between the states with $S = S_{gr}$. In the regarded compound we have $S_{gr} = 9/2$ and the energy gap between the states with different parity is equal to $2B(S_{gr} + 1/2) = 10B$.

$P(q)$, and the degree of delocalization, $\overline{\beta}_d^2$. The former value is the probability of finding the regarded system at a given nuclear configuration, q, and the latter is the measure of delocalization of the extra electron and lies between 0 (fully localized) and 1 (fully delocalized). For detail of calculations we refer to Ref. [17].

4. Discussion

Fig. 2 shows the intervalence absorption band for compound **2** calculated at low and room temperature. Increasing the temperature results in a shifting of the maximum point to the low-energy region, therefore the intervalence absorption band becomes less symmetric. One can assume that increasing the temperature results in localization degree increasing for compound **2**. The position and the shape of the calculated contour for compound **1** (not presented) are the same in this temperature region.

Let us start from the analysis of the adiabatic potentials of investigated systems (Fig. 3). The adiabatic potentials for compound **2** are asymmetric ones because of nonequivalent energies of Fe sites. However, for both compounds the adiabatic potentials look similar. Strong double exchange results in a ferromagnetic ground state for both complexes. For compound **1**, as well as for compound **2**, the $S = 9/2$ adiabatic curve possesses one minimum however, for non-centrosymmetric compound **2** this minimum corresponds to preferable localization of the extra electron at one of the Fe sites. So the ground vibronic state for compound **2** corresponds to a partially localized system, while for the other system, the ground state adiabatic curve minimum corresponds to a fully delocalized extra electron. Adiabatic potentials for other (smaller) values of the total spin of the system are higher in energy, possess two minima and correspond to excited states. While the value of the total spin decreases, the minima of the adiabatic curves become deeper and the barrier between them increases. For the $S = 1/2$ adiabatic curve we find two well-separated minima. Each of these minima corresponds to localization of the itinerant extra electron on one of two metal ions of the system, i.e. to a fully localized state. Besides the asymmetry of the adiabatic potentials for compound **2**, one can see another essential distinction: in compound **1** the ferromagnetic ground state is more isolated from the excited ones than in compound **2** because of the larger value of the double exchange parameter ($B = 820$ cm^{-1} compared to 600 cm^{-1}). The similarities and differences in the magnetic behaviour of the investigated compounds can be explained from this point of view. (The smaller value of the double exchange parameter in compound **2** can be explained by the fact that in this complex the distances between Fe ions and bridging ligands is larger than in compound **1**. These ligands also have an effect on the electron transfer process and thus on the values of the key parameters of the systems.)

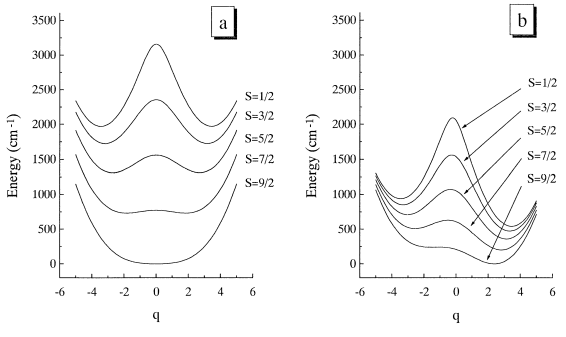

Fig. 3. Adiabatic potentials (low-lying group): (a) compound **1** ($B = 820$ cm^{-1}, $\omega = 310$ cm^{-1}, $\upsilon = 3.5\,\omega$, $J = -5$ cm^{-1}); and (b) compound **2** ($B = 600$ cm^{-1}, $\omega = 310$ cm^{-1}, $\upsilon = 3.5\,\omega$, $J = -22$ cm^{-1}, $W = 400$ cm^{-1}).

The values of the effective magnetic moments for both systems (Fig. 4) at low temperature (but > 30 K) indicate a ferromagnetic ground state. The sharp decrease of the magnetic moment below 30 K is explained by positive values of the axial component of the zero-field splitting tensor. In our calculation we found $D_{gr} = 3$ cm^{-1} for compound **1** and $D_{gr} = 4$ cm^{-1} for compound **2**. In the temperature region 50–300 K the effective magnetic moment of compound **1** depends slightly on the temperature. This is explained by the fact that a room temperature is still not high enough to populate the excited states with other (smaller) values of the total spin, and the magnetic properties of this system are still determined mostly by the well-isolated ferromagnetic ground state. In our calculation we obtained that the

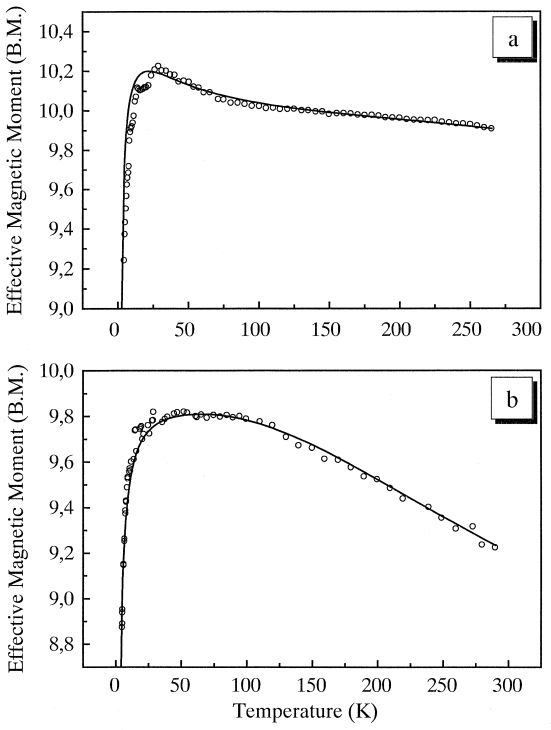

Fig. 4. Effective magnetic moments (open circles represent the experimental values, and solid curve is best fit obtained with: (a) $B = 820\ \mathrm{cm}^{-1}$, $J = -5\ \mathrm{cm}^{-1}$, $\omega = 310\ \mathrm{cm}^{-1}$, $\upsilon = 3.5\,\omega$, $D_{\mathrm{gr}} = 3\ \mathrm{cm}^{-1}$, $g_{\|} = 1.73$, $g_{\perp} = 2.11$ (compound **1**); and (b) $B = 600\ \mathrm{cm}^{-1}$, $J = -22\ \mathrm{cm}^{-1}$, $\omega = 310\ \mathrm{cm}^{-1}$, $\upsilon = 3.5\,\omega$, $D_{\mathrm{gr}} = 4\ \mathrm{cm}^{-1}$, $g_{\|} = 1.93$, $g_{\perp} = 1.99$ (compound **2**)).

relative population of the first excited $S = 7/2$ adiabatic curve minima at room temperature is $< 2.9\%$ (in Ref. [10] this value was evaluated to be $< 1\%$). The same estimations for compound **2** show that at room temperature the relative population of the $S = 7/2$ adiabatic curve minima is $\sim 38\%$, for the $S = 5/2$ adiabatic potential this value is $\sim 18\%$, etc. So the thermal population of the excited spin multiplets becomes significant and comparable with the population of the ground multiplet. This results in the temperature behaviour of the effective magnetic moment.

Fig. 5a shows the probability distribution in the configuration space for compound **1** at low and at room temperature. For both cases the probability distribution, $P(q)$, has a single maximum at $q = 0$. It corresponds to the most probable configuration in which both subunits are equivalent and have the equal oxidation degree. This is the untrapped (or delocalized) case. Compound **1** belongs to Class III in the Robin and Day classification scheme. For compound **2** the situation is more complicated. Fig. 5b shows the probability distribution in the configuration space for this system. At low temperature, $P(q)$ also has a single maximum but this maximum corresponds to the situation when the Fe subunits have different oxidation degrees. The extra electron is partially localized. At room temperature $P(q)$ has two maxima, each corresponding to the situation when one of the Fe ions is in a $+2$ state and the other in a $+3$ one. It is the valence trapped (or localized) case. Nevertheless, the probability of finding the system in a configuration with equal oxidation of subunits is non-zero. Respective degrees of delocalization of the extra electron calculated after Ref. [17] are $\overline{\beta}_d^2 = 0.58$ at $T = 30$ K and $\overline{\beta}_d^2 = 0.55$

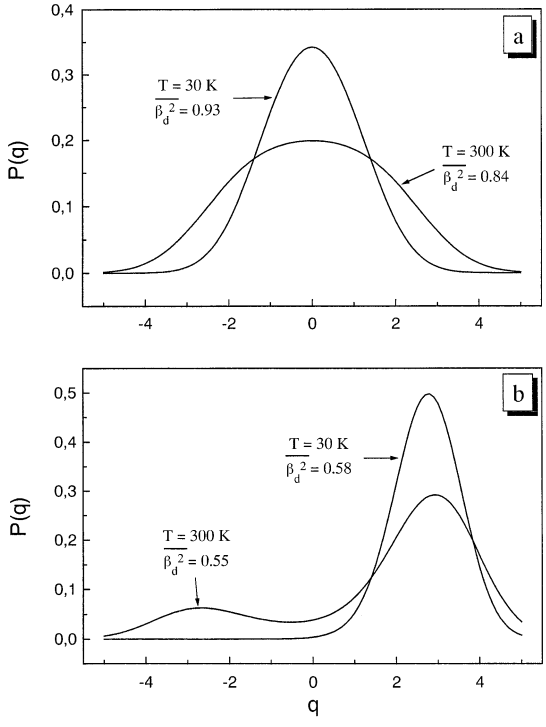

Fig. 5. Probability distribution in configuration space at low and room temperature for compound **1** (a) and compound **2** (b). Degree of delocalization of the extra electron is shown near the corresponding curves.

at $T = 300$ K (for compound **1** these values are $\overline{\beta}_d^2 = 0.93$ at $T = 30$ K and $\overline{\beta}_d^2 = 0.84$ at $T = 300$ K).

Decreasing $\overline{\beta}_d^2$ while the temperature increases can be explained using the adiabatic potentials of the regarded compounds. The degree of delocalization of the extra electron is a spin-dependent value. The adiabatic curve for the $S = 9/2$ state has a single minimum for both compounds and corresponds to the fully delocalized case (compound **1**) or partially localized one (compound **2**). While the total spin value decreases, the minima of the adiabatic curves become deeper, which leads to the trapping of the itinerant extra electron. A smaller value of the total spin corresponds to a smaller value of the degree of delocalization. That is why the thermal population of the excited states with smaller values of the total spin leads to decrease of the delocalization degree of the extra electron. At room temperature the thermal population of the excited states for compound **2** is significant and it becomes more and more localized, meanwhile the behaviour of compound **1** is still determined by the ferromagnetic ground state only and the extra electron remains fully delocalized.

5. Summary

The behaviour of both compounds is determined by a strong competition between two processes: double exchange interaction and vibronic coupling with the PKS out-of-phase mode. The former leads to delocalization of the itinerant electron while the latter represents a trapping effect that tends to localize the extra electron.

Strong double exchange results in a ferromagnetic ground state for both complexes. However, in compound **1** this state is more isolated from the excited ones than in compound **2** because of the large value of the double exchange parameter.

At low temperature the behaviour of both systems is determined by the ferromagnetic ground state only and compound **1** is fully delocalized. In compound **2** there is some additional extra electron localization effect because of non equivalency in energy of two interacting ions. At low temperature the extra electron in this compound is partially localized. At room temperature the behaviour of compound **1** is still determined by the ferromagnetic ground state and it remains mostly delocalized, meanwhile for compound **2** the thermal population of the excited states plays a significant role and the itinerant extra electron becomes more and more localized.

Acknowledgements

Authors are grateful to Professor B.S. Tsukerblat for very fruitful discussions. We thank the Deutsche Forschungsgemeinschaft (DFG) for financial support.

References

[1] E.L. Bominaar, C. Achim, S.A. Borshch, J.-J. Girerd, E. Münck, Inorg. Chem. 36 (1997) 3689.
[2] C. Achim, E.L. Bominaar, E. Münck, J. Bioinorg. Chem. 3 (1998) 126.
[3] V. Papaefthymiou, J.-J. Girerd, I. Moura, J.J.G. Moura, E. Münck, J. Am. Chem. Soc. 109 (1987) 4703.
[4] L. Noodleman, D.A. Case, Adv. Inorg. Chem. 38 (1992) 423.
[5] D.R. Gamelin, E.L. Bominaar, M.L. Kirk, K. Wieghardt, E.I. Solomon, J. Am. Chem. Soc. 118 (1996) 8085.
[6] D.R. Gamelin, E.L. Bominaar, C. Mathoniere, M.L. Kirk, K. Wieghardt, J.-J. Girerd, E.I. Solomon, Inorg. Chem. 35 (1996) 4323.
[7] S. Drüeke, P. Chaudhuri, K. Pohl, K. Wieghardt, X.-Q. Ding, E. Bill, A. Sawarin, A.X. Trautwein, H. Winkler, S.J. Gurman, J. Chem. Soc., Chem. Commun. (1989) 59.
[8] X.-Q. Ding, E.L. Bominaar, E. Bill, H. Winkler, A.X. Trautwein, S. Drüeke, P. Chaudhuri, K. Wieghardt, J. Chem. Phys. 92 (1990) 178.
[9] X.-Q. Ding, E. Bill, A.X. Trautwein, H. Winkler, A. Kostikas, V. Papaefthymiou, A. Simopoulos, P. Beardwood, J.F. Gibson, J. Chem. Phys. 99 (1993) 6421.
[10] C. Saal, S. Mohanta, K. Nag, S.K. Dutta, R. Werner, W. Haase, E. Duin, M.K. Johnson, Ber. Bunsen-Ges. Phys. Chem. 100 (1996) 2086.
[11] S.K. Dutta, J. Ensling, R. Werner, U. Flörke, W. Haase, P. Gütlich, K. Nag, Angew. Chem. 109 (1997) 107.
[12] C. Saal, Ph.D. Thesis, Technische Universität Darmstadt, Darmstadt, 1998.
[13] C. Zener, Phys. Rev. 82 (1951) 403.
[14] P.W. Anderson, H. Hasegawa, Phys. Rev. 100 (1955) 675.
[15] S.B. Piepho, E.R. Krausz, P.N. Schatz, J. Am. Chem. Soc. 100 (1978) 2996.
[16] P.N. Schatz, in: D.B. Brown (Ed.), Mixed-Valence Com-

pounds, NATO Adv. Stud. Inst. Ser., Reidel, Dordrecht, 1980, p. 115.
[17] K.Y. Wong, P.N. Schatz, Prog. Inorg. Chem. 28 (1981) 369.
[18] S.B. Piepho, J. Am. Chem. Soc. 110 (1988) 6319.
[19] S.B. Piepho, J. Am. Chem. Soc. 112 (1990) 4197.
[20] M.B. Robin, P. Day, Adv. Inorg. Radiochem. 10 (1967) 247.
[21] J.J. Borras-Almenar, E. Coronado, S.M. Ostrovsky, A.V. Palii, B.S. Tsukerblat, Chem. Phys. 240 (1999) 149.
[22] To be published.
[23] S. Gehring, P. Fleischhauer, H. Paulus, W. Haase, Inorg. Chem. 32 (1993) 54.
[24] O. Kahn, Molecular Magnetism, VCH, Weinheim, 1993.